

## Advanced Techniques for Navigation Receivers and Applications

# ATENEA

## D10.3 – Executive Summary



*ATENEA: Hitting Advanced Positioning Techniques*

**Code :** ATENEA-DMS-TEC-FIR02-E-R

**Issue :** 1.2

**Date :** 20/07/2012

	Name	Function	Signature
Prepared by	Antonio Fernández	Project Manager	
Reviewed by	Antonio Fernández	Project Manager	
Approved by	Antonio Fernández	Project Manager	

*Signatures and approvals on original*

DEIMOS Space S.L.U.  
Ronda de Poniente, 19  
28760 Tres Cantos (Madrid), SPAIN  
Tel.: +34 91 806 34 50 / Fax: +34 91 806 34 51  
E-mail: deimos@deimos-space.com





## Document Information

Contract Data	
Contract Number:	TREN/FP/TR/247975
Contract Issuer:	EC-DG TREN

Distribution	
Name	Organisation
Antonio Fernández	DMS
José Diez	DMS
Augusto Caramagno	DMS
Joachim Lindenberger	TopScan
Fabio Dovis	POLITO
Pedro F. Silva	DME
Eulàlia Pares	IG
Ismael Colomina	IG
Peter Friess	GEONUM
Ignacio Fernández	EC

Confidentiality Level <sup>1</sup>			
PU	<input type="checkbox"/>	PP	<input checked="" type="checkbox"/>
RE	<input type="checkbox"/>	CO	<input type="checkbox"/>

Archiving	
Word Processor:	MS Word 2007
File Name:	ATENEA-DMS-TEC-FIR02-12-E-R_D103_Executive Summary_v1.2.doc

<sup>1</sup> As defined in [AD-1]:

**PU** = Public

**PP** = Restricted to other programme participants (including the GSA).

**RE** = Restricted to a group specified by the Consortium (including the GSA).

**CO** = Confidential, only for members of the Consortium (including the GSA).



## Document Status Log

Issue	Change description	Date	Approved
1.0	First Version	13/03/12	
1.1	Minor updates	27/03/12	
1.2	Update after Final Review	20/07/12	



## Table of Contents

<b>1. Introduction</b>	<b>5</b>
1.1. The ATENEA project	5
1.2. Purpose and scope	6
1.3. Acronyms and Abbreviations	6
1.4. Applicable Documents	7
1.5. Reference Documents	7
<b>2. Executive summary</b>	<b>9</b>
2.1. Summary description of project contents and objectives	9
2.2. Description of the main S&T results / foregrounds	10
2.2.1. Summary	10
2.2.2. Application and User Analysis	11
2.2.3. Galileo Signal Processing	14
2.2.4. Deep Integration Analysis	15
2.2.5. ATENEA Platform	19
2.2.6. VALIDATION	23
2.3. Conclusions	32
2.4. Public website address and relevant contact details	32

## List of Figures

Figure 1: Mobile Imaging example: Transmap Mobile Mapping System	12
Figure 2: Optech Lynx operated by TopScan GmbH (www.topscan.de)	12
Figure 3: Optimum orientation of 2 LiDAR sensors (www.optech.ca)	12
Figure 4: Mobile Laserscanning project with high accuracy requirements	13
Figure 5: Mobile Laserscanning along the riverbank for flood modelling	13
Figure 6: Level 4 – Tightly coupled hybrid GNSS-INS architecture	15
Figure 7: Level 5 – Ultra-Tightly coupled hybrid GNSS-INS architecture	16
Figure 8: Level 5 – Ultra-Tightly coupled hybrid GNSS-INS performances	18
Figure 9: ATENEA Platform concept	19
Figure 10: Imported building environment (right) from Google Earth models (left)	20
Figure 11: LiDAR processing for integration in the navigation filter	22
Figure 12: Point cloud resulting of the LiDAR scanning and plane location	22



Figure 13: Plane matching.....	22
Figure 14: NAVEGA filter architecture .....	22
Figure 15: Experimental receiver (top) and receiver model (bottom) .....	23
Figure 16: Urban Canyon Scenario (S2 in Table 5) .....	24
Figure 17: Imported Field test data collection campaign path .....	25
Figure 18: TopScan experimental setup .....	25
Figure 19: Collected LiDAR data.....	26
Figure 20: Example of LiDAR pre-processed data from Dortmund campaign after the primary plane extraction (left) and extracted geometrical planes (right) .....	26
Figure 21: ACF derivation from IF data.....	26
Figure 22: simulations results in sub-urban environment.....	27
Figure 23: simulations results in urban environment. ....	28
Figure 24: low cost sensors simulations .....	29
Figure 25: results from real datasets.....	30
Figure 26: Part of the track in which multipath was found (red points).....	31

## List of Tables

Table 1: Applicable Documents .....	7
Table 2: Summary of ATENEA improvements over state of the art .....	10
Table 3: Expected aided receiver performances based on code observables.....	17
Table 4: Expected aided receiver performances based on code observables.....	18
Table 5: Validation Scenarios (synthetic data).....	24

# 1. INTRODUCTION

## 1.1. The ATENEA project

Urban mapping by LIDAR images is an active research domain, but today it is only viable by using high-end systems with a cost per unit in the order of 800 K€. In addition, LIDAR device geolocation and reference for the scanned observables is provided nowadays by loosely coupled GPS/INS receivers, degrading performance in urban scenarios with poor satellite visibility and harsh multipath conditions.

ATENEA tackles the most challenging issues of this type of applications, showing how the use of GNSS signals, integrated positioning and observable processing can in one shot increase robustness, continuity, accuracy and drastically reduce the system cost. The ATENEA project has developed an advanced concept for seamless navigation at the cm-level regardless of the environment based on the following technologies:

- **Deeply coupled GNSS/INS receiver design.** Current state-of-the-art of hybridisation applications are improved with ultra-tight integration of the inertial sensors, navigation processor and signal processing tracking loops, adding additional robustness under high user dynamics and SIS signal blockages. The test campaign has shown that in urban environments there is a clear improvement in the navigation solution for tightly coupled approaches.
- **Galileo signal capabilities.** Errors in the pseudorange observables are reduced by using dedicated signal processing techniques taking benefit of the Galileo E1 MBOC and E5 AltBOC signals. The **Galileo E5AltBOC signal offers excellent performances in all conditions** (open sky, shadowed and multipath). This modulation opens a field for professional GNSS applications with unprecedented accuracy.
- **Integrated GNSS/INS/LIDAR navigation filter.** Finally, an innovative unique integrated navigation solution for the integration of observables from GNSS, IMU, and laser sensors is proposed, allowing to reduce the costs of the currently expensive equipment in these applications. The use of LiDAR measurements in the navigation filter results in a huge increase of performance in urban environment, especially in the horizontal component. The approach for LiDAR integration in the navigation filter derived in ATENEA, that to the knowledge of the authors has not been used previously (using LiDAR identified planes as boundary condition), has been proofed optimum.

The proposed algorithms have been tested in the ATENEA platform SW environment, developed upon the GRANADA simulator and the IADIRA test-bench (results from GJU projects lead by DEIMOS). A field campaign with real data has been carried out. The ATENEA technologies have been thus investigated down to a pre-industrialized solution ready to be integrated in professional applications.

The expected impact of the ATENEA technology is related to the ability to navigate at a  $1\text{-}\sigma$  accuracy level ranging from 0.05 to 0.50 m in urban areas. This capacity is an enabler for numerous outdoor –and even some indoor– applications, and is the result of integrating three different, mutually complementary technology principles: GNSS ranging, inertial sensing and LiDAR ranging.

Among other applications, the technology developed under ATENEA is key for the third generation mapping paradigm, terrestrial mobile mapping: 3D Earth surface models that will include 3D urban city models. 3D models of the Earth surface must be elaborated by combining data from aerial/satellite and terrestrial missions. ATENEA is the enabler for the terrestrial geodata acquisition missions.

The project has been led by DEIMOS Space. As partners, IG and DME provide their expertise in GNSS/INS hybridisation, while the Politecnico of Torino and GeoNumerics have wide experience in GNSS signal processing and LiDAR, respectively. TopScan provided the user point of view.



## 1.2. Purpose and scope

This document represents the Executive Summary for ATENEA, covering results, conclusions and socio-economic impact of the project.

## 1.3. Acronyms and Abbreviations

A/D	Analog-to-Digital
ACF	Autocorrelation Function
AltBOC	Alternate Binary Offset Carrier
BPSK	Binary Phase Shift Keying
BOC	Binary Offset Carrier
BW	Bandwidth
CBOC	Composite Binary Offset Carrier
DLL	Delay Lock Loop
DME	DEIMOS Engenharia
DMS	DEIMOS Space
DOP	Dilution of Precision
EU	European Union
ESA	European Space Agency
FOC	Full Operational Capability
GEONUM	GeoNumerics
GIOVE	Galileo In-Orbit Validation Element
GJU	Galileo Joint Undertaking
GKMF	Galileo Knowledge Management Facility
GNSS	Global Navigation Satellite System
GPS	Global Positioning System
GRANADA	Galileo Receiver Analysis and Design Application
GSA	GNSS Supervisory Authority
ICD	Interface Control Document
IF	Intermediate Frequency
IG	Institute of Geomatics
IGS	International GNSS Service
IOV	In-Orbit Validation
KOM	Kick-Off Meeting
LiDAR	Light Detection and Ranging
MBOC	Multiplexed Binary Offset Carrier
MMS	Mobile Mapping System
NELP	Non-coherent Early-Late Processing
OD&TS	Orbit Determination & Time Synchronisation
PLL	Phase Lock Loop
PPP	Precise Point Positioning
POLITO	Politecnico di Torino
RAIM	Receiver Autonomous Integrity Monitoring
RF	Radio Frequency
RTK	Real-Time Kinematic
S/C	Space Craft
S/T	Scientific & Technical





SIS	Signal-In-Space
SMR	Signal-to-Multipath Ratio
SW	Software
TMBOC	Time Multiplexed Binary Offset Carrier
TMMS	Terrestrial Mobile Mapping System
UERE	User Equivalent Range Error
WBS	Work Breakdown Structure
WP	Work Package

## 1.4. Applicable Documents

Ref.	Title
[AD-1]	Description of Topic Galileo.2008.3.1.4. Professional Receivers. 7 <sup>th</sup> FP of the European Community for Research, Technological Development, and Demonstration Activities (2007 to 2013). 'Cooperation Specific Programme'.
[AD-2]	Guide for Applicants. Theme 7: Transport (including Aeronautics). Collaborative Project. Ref: FP7-GALILEO-2008-GSA-1.
[AD-3]	ATENEA description of work; part B: Ref. ATENEA-DMS-COM-PRL01-R; issue 1.2; 22/11/2009

**Table 1: Applicable Documents**

## 1.5. Reference Documents

- [1] Novak, "The Ohio State University Mapping System: The Stereo Vision System Component", Proceedings of the 47th Annual Meeting. The Institute of Navigation (ION), pp 121-124, 1991
- [2] Cameron Ellum and Nasser El-Sheimy "Land-Based Mobile Mapping Systems" PE&RS January 2002 pp. 13-18
- [3] Bossler and Toth, "Feature Positioning Accuracy in Mobile Mapping Results obtained by the GPSVan<sup>TM</sup>", Int. Archives of Photogrammetry and Remote Sensing, Vol. XXXI, Part B4, Vienna 1996.
- [4] Dovis F.; Lo Presti L; Fantino M; Mulassano P; and Godet J, "Comparison Between Galileo CBOC Candidates and BOC(1,1) in Terms of Detection Performance", INTERNATIONAL JOURNAL OF NAVIGATION AND OBSERVATION, 2008, Vol. 2008
- [5] E. Falletti, D. Margaria, B. Motella, "Educational Library of GNSS Signals for Navigation", Coordinates, Issue 8, Vol. V, pp.30-34, ISSN: 0973-2136, August 2009.
- [6] Silva, P. et al., "Evaluating Receiver Architectures for Inertial Aiding and Coasting", ION GNSS 2007, September 2007, Fort Worth, Texas
- [7] Kreye, C. Eissfeller, B. , et al., "Performance Analysis and Development of a Tightly Coupled GNSS/INS System", 9th St. Petersburg International Conference on Integrated Navigation Systems, May 2002, St. Petersburg, Russian Federation
- [8] Li D., Wang J., "System Design and Performance Analysis of Extended Kalman Filter-Based Ultra-Tight GPS-INS Integration", IEEE/ION PLANS 2006, April 2006, Coronado (San Diego), California
- [9] J. Betz, K. Kolodziejewski, "Generalized Theory of Code Tracking with an Early-Late Discriminator. Part II: Noncoherent Processing and Numerical Results," IEEE Trans. on Aerospace and Electronic Systems, vol. 45, pp. 1551-1564, October 2009
- [10] J.S. Silva, P.F. Silva, A. Fernández, J. Diez, J.F.M. Lorga, "Factored Correlator Model: A Solution for Fast, Flexible, and Realistic GNSS Receiver Simulations", Proceedings of ION GNSS 2007, Fort Worth (Texas).
- [11] Soloviev, A., 2008. Tight Coupling of GPS, Laser Scanner, and Inertial Measurements for Navigation in Urban Environments. 1-4224-1537-3/08, 2008 IEEE.
- [12] GNSS Market Report, Issue 1, October 2010, Galileo Supervisory Authority
- [13] "Business Outlook: Precision Market to Reach \$8B by 2012", GPS World, November 2008, <http://www.gpsworld.com/survey/news/business-outlook-precision-market-reach-8b-2012-3695>



Intentionally left blank



## 2. EXECUTIVE SUMMARY

### 2.1. Summary description of project contents and objectives

The goal of the ATENEA project is to:

- *Develop an advanced technology concept for seamless navigation at the cm-level regardless of the environment.*
- *Integrate the complementary capabilities of GNSS, inertial navigation and object feature-based navigation from LiDAR sensors*
- *Demonstrate the concept by implementing the developed algorithms in a dedicated SW simulation platform*
- *Perform a validation campaign focused on urban environment, including both synthetic and real measurements.*

As summary, ATENEA develops innovative solutions not available in current receivers: specific exploitation of Galileo signal capabilities; innovative signal processing techniques; closely, tightly and deeply coupled GNSS/INS receiver design; integrated GNSS/INS/LiDAR navigation filter.

ATENEA concept is at the same time innovative and very oriented to actual user needs, providing a unique enabler for user market in professional receiver and integrated systems.



## 2.2. Description of the main S&T results / foregrounds

### 2.2.1. Summary

The following technologies are developed within the ATENEA project, providing innovative solutions not available in current receivers:

- *GNSS Phase receiver, exploitation Galileo signals capabilities*
- *Innovative signal processing techniques*
- *Closely, tightly and deeply coupled GNSS/INS receiver design*
- *Integrated GNSS/INS/LiDAR navigation filter.*

The following table summarises the pros and cons of each of the considered techniques for Urban Mapping applications, highlighting the benefits of an integration solution.

<i>Urban Environments</i>	<b>Precision</b>	<b>Accuracy</b>	<b>Continuity</b>	<b>Multipath error</b>	<b>Positioning</b>	<b>Nav. Equipment Price</b>
<b>GPS</b>	~ 10 m	~ 10 m	Low	~ 5 m	Absolute	~200 €
<b>Galileo/EGNOS/GPS</b>	~ 2 m	~ 2 m	Medium	~ 1 m	Absolute	~300 €
<b>INS</b>	~ 50 cm	~ 100 m	High	No	Relative	1 – 10 K€
<b>GNSS/INS</b>	~ 1 cm	~ 50 cm	Very High	~ 50 cm	Absolute	10 – 100 K€
<b>LiDAR</b>	~ 20 cm	~ 100 m	High	No	Relative	1 – 1000 K€
<b>ATENEA</b>	~ 5 cm	~ 5 cm	Very High	~ 10 cm	Absolute + Relative	10 – 50 K€

**Table 2: Summary of ATENEA improvements over state of the art**

In addition, the ATENEA SW test-bench developed for algorithm validation is a valuable asset of the project, providing a development environment for Multisensor Navigation Systems integrating GNSS and other sensors such as INS or LiDAR.



### **2.2.2. Application and User Analysis**

Mobile Mapping became a keyword in surveying and geo-informatics in the past three years. Mobile Mapping describes a new approach in these technologies with very high impact on wide user applications; this technology is characterized by acquisition of data from a moving vehicle. Although the application of ATENEA technology may have a wide potential on very different applications, including mass market / consumer applications, the focus of ATENEA is on high precise mobile mapping.

The data acquisition sensor can be digital RGB camera or LiDAR. Mobile Mapping is not limited on these two sensor types; depending on the application other sensors like thermal camera, hyper-spectral sensors, or combinations of different sensors are in operation.

One or more digital RGB cameras are the characterizing sensors for Mobile Imaging Systems. Mobile Imaging Systems were the earliest realizations of Mobile Mapping Systems. The earliest experimental system known under the trade name GPSVanTM, which was realized at the Ohio State University in the early 1990<sup>th</sup> [1]. Later, the experimental system led in a commercial success under Transmap Corp (Figure 1).

For geo-referencing of the sensor data [2], the GPSVanTM uses GPS for positioning, 2 odometers for positioning support bridging GPS outages, and 2 gyros for orientation. In the later, commercial version, the gyros were replaced by IMU.

Two frame cameras do the mapping, both front looking with overlapping field of view to enable stereographic mapping in the image pairs. Starting from monochrome CCD frame cameras with VGA resolution, today RGB frame cameras with HD resolution (2MPixel) are used.

The bridging of outages of satellite signal reception was the main problem for precise mapping, leading to more expensive hardware device for navigation by using INS. One of the core ideas of ATENEA, the integration of additional orientation data into the GNSS/INS Kalman filter process, was not seriously pursued.

After having analyzed data from 9000km street survey and 2000km from rail tracks, an average planimetric error of 50cm is reported in [3], where the dominant part is caused by the geo-referencing. This limited accuracy restricts the range of applications to a number of applications, with less demanding accuracy requirements. High precision mapping, with accuracy requirements of better than 1dm, is not done by imaging sensors, but is the domain of LiDAR systems,

The development of the Mobile Imaging technology and market was and still is driven by individual companies or institutions. In contrary to Mobile Laserscanning, no hardware manufacturer offers a complete, standardized Mobile Mapping system. Thus, there exist a big number of individual vehicles, designed mainly by the system operating company and optimized for their specific applications. While a big number of small service provider companies operate a small number of systems (typically 2 systems), there exist a small number of big companies (like Google, Navteq, Tele Atlas) operating a larger fleet of similar vehicles.

Mobile Laser scanning Systems is a considerably younger technology, the first complete integrated system was released by the Canadian company Optech Inc. in 2007. The market is dominated by a few LiDAR system manufacturers offering complete turnkey solutions, operating typically only one system, specialized in a certain number of applications. Recent evolution tends toward an integration of imaging sensors for documentation and support of interpretation of the LiDAR data. Mobile Laserscanning rules the market of high precision Mobile Mapping.



**Figure 1: Mobile Imaging example: Transmap Mobile Mapping System**

Optech is the market-leading. Their Lynx system follows a modular concept giving the customer the choice to select up to 4 LiDAR sensors and offers different geo-referencing sub-systems. Optionally up to actual 2 (in future 4) digital cameras with 2 or 5 Mpixel of resolution can be selected. The camera data is time-tagged and recorded together in the central control computer. Nevertheless, a kind of standard configuration is selected with 2 LiDAR sensors and the Applanix LV 420 GPS/INS sub-system. TopScan GmbH operates one of these constellations since 2008 (Figure 2). This system has been used in the ATENEA field test campaign.

The introduction of features derived from LiDAR data into the Kalman filtering process to improve positioning requires a high point density to be able to extract object features and reliably match them in a second data set, and extracted object features taken from two different points in time, but within the same trajectory. Fig. 2 shows the installation of the LiDAR sensors in the corner of the mounting platform. This distinct orientation with 45deg angle to the trajectory was originally proposed to enable a maximum coverage of the object space by laser points and to avoid occlusions (Figure 3).

The impact of the selected orientation of the LiDAR sensors for ATENEA is that within a short time objects are scanned twice on the same drive. Assuming a speed of 30km/h, each object in 20m distance to the sensor will be scanned a second time after 5 seconds. The effect of a drift of the positioning system can clearly be visualized as shift between the point clouds of the two sensors.



**Figure 2: Optech Lynx operated by TopScan GmbH ([www.topscan.de](http://www.topscan.de))**

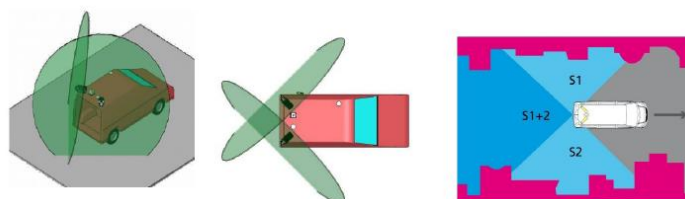


**Figure 3: Optimum orientation of 2 LiDAR sensors ([www.optech.ca](http://www.optech.ca))**





Applications can be categorized into three groups according to their accuracy requirements: high, medium and low.

$\sigma < 50\text{cm}$ : low accuracy requirement.

Under this category, we find navigation applications such as data acquisition for navigation products such as consumer car navigation (eg NAVTEQ or TeleAtlas); map visualization applications such as Google's trademark 'Streetview'; or street pavement management, monitoring the condition of the pavement of major roads.

$\sigma < 15\text{cm}$ : medium accuracy requirement

Applications include public asset management or photorealistic 3-D city modes; these models have a very broad prominence, again caused by the public presentation in the Internet and especially Google Earth.

$\sigma < 5\text{cm}$ : high accuracy requirement

Two main applications have been identified. The first one is cadastral mapping, which demands very high accuracy (a standard deviation of  $<3\text{cm}$  is required). Figure 4 shows a colorized point cloud including vectorized objects of a typical project, in main narrow through-road through an old village.

The high accuracy only can be reached with additional control points, determined by stationary GPS measurements or traditional surveying methods. The reduction of number of additional control points, by advanced positioning technique like ATENEA, will drastically reduce the effort and the costs for high precise Mobil Mapping.

The second application, Figure 5, is mapping for flood modeling, which does not have such high accuracy requirements (typical standard deviation is  $5\text{cm}$ ).



**Figure 4: Mobile Laserscanning project with high accuracy requirements**

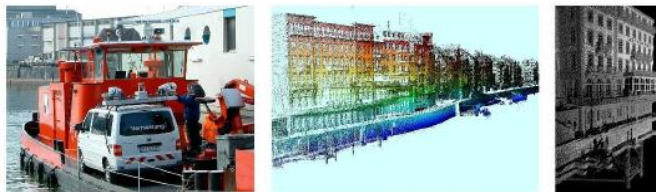


**Figure 5: Mobile Laserscanning along the riverbank for flood modelling**



### 2.2.3. Galileo Signal Processing

In the course of ATENEA, research has been performed in specific technologies improving the state-of-the-art of current GNSS receivers. Focus of the research have been signal processing analysis of Galileo L1 MBOC and E5 signals; interference mitigation; and integrated navigation filter, for which different levels of hybridization have been considered.

#### ▪ MBOC acquisition and tracking

MBOC represents one of the main innovations of the new generation of GNSS. Its impact on the receiver architectures (i.e. filter band requirements) or on legacy receivers has been widely studied (see eg [4]). Several techniques have been analyzed for MBOC acquisition and tracking:

- Conventional single channel (SC) acquisition strategy.
- Joint Data / Pilot MBOC acquisition strategies
- Post Correlation Differential Signal processing, in conventional or generalized differential combinations

The techniques have been analysed theoretically in terms of false alarm probability and mean acquisition time. They have been also prototyped in the Full Educational Library of Signals for Navigation (N-FUELS©) SW receiver developed by the NavSAS group [5]. From the performance evaluation results, the stand-alone joint strategies prove their advantages over the conventional SC strategy. Specifically, the improvement of 2.8 (dB) is granted to the stand-alone joint strategies when one full code period is considered. If non-coherent combination is used, this improvement reduces, e.g. 1.8 (dB) if 50 code periods are considered, because of the squaring loss phenomenon.

#### ▪ AltBOC acquisition and tracking

As far as the possible receiver architectures for the E5 signals are concerned, they can be essentially grouped into two categories: the BPSK-like or the true AltBOC architectures.

Being originally tailored for a Safety-of-Life service, the AltBOC signal may be out of the set of possible signals for a conventional receiver. However, the original modulation scheme and the challenging complexity of processing it makes worth to consider some low complexity schemes that may be applied also to some other Galileo signals. In particular, two recently proposed techniques tailored to AltBOC signals have been identified as good candidates, since they are a good trade-off between complexity and performance:

- the multiresolution acquisition strategy, based on a signal search performed in multiple steps
- the solution based on the Side-Band Translator (SBT), a novel data demodulation technique under patent.

Both techniques have been analysed in depth and prototyped in the N-FUELS SW receiver. In summary both strategies can be considered as good trade-offs between complexity and performance and in this sense they are suitable to a professional receiver.



### 2.2.4. Deep Integration Analysis

Current LIDAR systems for geolocation and reference purposes use GPS receivers and INS in a closely coupled approach, with no feedback of the INS to the receiver tracking loops. This leads to lack of performance in urban scenarios with poor satellite visibility and harsh multipath conditions. In the course of ATENEA, higher integration levels for tightly coupled approach have been assessed:

#### ▪ Tightly Coupled Architecture (Level 4)

In the tightly coupled architecture [6], [7], the integration filter receives raw measurements from both GNSS and inertial sensors, as depicted in Fig. 6. The GNSS receiver provides pseudorange, carrier phase and rate measurements as well as navigation data from which to derive satellite positions, and the IMU provides accelerations and angular rates. All these measurements are fed to the integration filter and there is no longer the need for the GNSS and inertial navigators. However, in this architecture, inertially derived data is fed back from the integration filter to the GNSS tracking loops to aid GNSS signal tracking, estimating the Doppler shift that the receiver is experiencing. This reduces the loops' dynamic stress and allows the reduction of the loops bandwidths, resulting in an increased robustness to interference, dynamics, signal blockage, and in a reduction of the GNSS measurements noise. This high level of integration may have some draw backs: aiding quality also depends on navigation solution quality, and access to the receiver signal processing stage is mandatory; in addition, care must be taking with clock oscillator noise and with multipath. In our architecture, all the navigation processing is done in the integration filter, which estimates also the inertial sensor errors, such as biases and misalignments.

Figure 6 shows a block diagram of a receiver tracking stage using tight integration. A carrier tracking loop (orange) tracks the carrier phase and/or frequency and a code tracking loop (yellow) tracks the code phase. The navigation solution from the Kalman Filter is used for aiding of the tracking stage, shown as the line that connects the carrier tracking loop with the Kalman filter. The carrier and code tracking loops produce estimates of the carrier and code phases (respectively), which are used to steer the local carrier generator and chip accumulator blocks

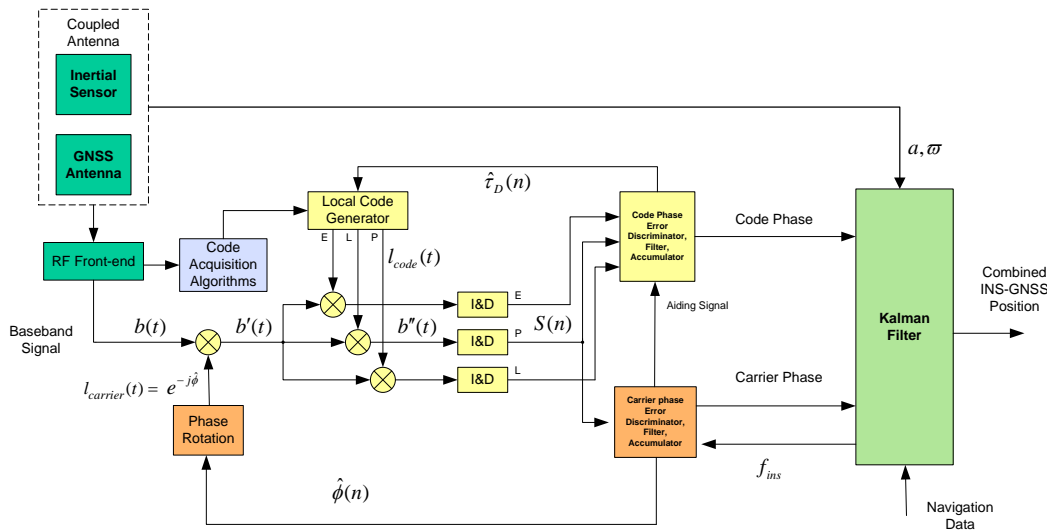


**Figure 6: Level 4 - Tightly coupled hybrid GNSS-INS architecture**

### ▪ Ultra-Tightly Coupled Architecture (Level 5)

The integration filter in the ultra-tightly coupled architecture, [8], [7], illustrated in Figure 7, uses even deeper (rawer) GNSS measurements than in the previously described integration architectures. The ultra-tight configuration uses the vector tracking technique such as in the tight configuration in the sense that the outputs of the navigation filter are used by tracking loops. However, this approach, the discriminators are removed; hence individual tracking loops are replaced by the navigation filter. This allows the bandwidth adaptation to everything that is modelled by the Kalman filter, including INS and clock dynamics, which can lead to substantial performance improvements. Several approaches for system and measurement models are reported in [9].

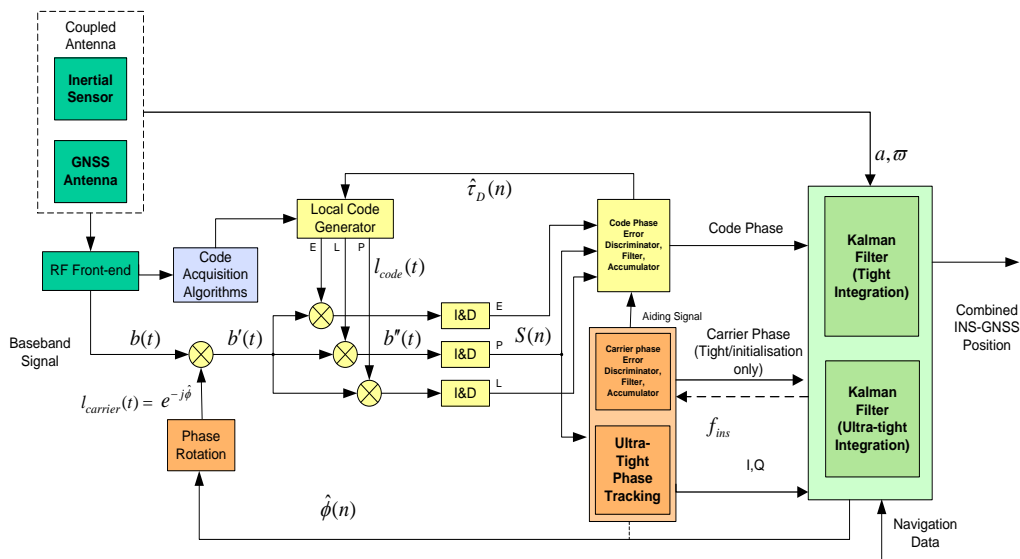


**Figure 7: Level 5 - Ultra-Tightly coupled hybrid GNSS-INS architecture**

Both approaches have been implemented in a SW simulator based on the GRANADA Factor Correlator Model [10]. The computation load of Level 5 integration is higher since Kalman Filter is required for processing the correlator outputs, when compared to a simple discriminator. Computational load of ultra-tight integration can be substantially reduced using cascaded, multirate when compared to direct use of I and Q, hence computation load is not expected to be a problem. However, new receiver control logic and operation procedures need to be developed.

The influence of several parameters has been analyzed: number of usable satellites, signal modulation, loop bandwidth, inertial sensor quality, integration times and oscillator quality.

For Level 5 integration, a study of tracking sensitivity of the filter to lower grade inertial sensor and oscillator quality with respect to tight integration has been performed.

Simulation results shows that for the DLL, the measurement noise decreases when the bandwidth decreases, reaching an inversion point at approximately 2.5 Hz without aiding and 0.2 Hz in the case of aiding. Since the DLL is rate aided by the PLL as long as the PLL is correctly tracking the signal, a value of 0.5 Hz shall be assumed as the baseline, with a corresponding error below 0.4 and 1 m for a  $C/N_0$  of 45 and 30 dB-Hz respectively in the case of Galileo E1 signal. When AltBOC(15,10) is used together with an aiding signal, code observation errors reach 0.1 m for a  $C/N_0$  of 30 dB-Hz which could be a more interesting solution, as it allows better positioning performances either absolute or differential (e.g. faster solution convergence in the case of RTK, more accurate code smoothed carrier phase).

In the case of the PLL, the observable noise is always higher than in the case of aiding but with decreasing differences for higher bandwidths. As shown in 0 below, for a PLL equivalent bandwidth of 40 Hz and



without aiding, the carrier phase error reaches 2 mm and 7 mm for a  $C/N_0$  of 45 and 30 dB-Hz respectively, while if aiding is used the errors reach 1 mm and 6 mm respectively for that same filter bandwidth. However, thanks to aiding, values of 1 mm and 3 mm can be reached if a bandwidth of 8Hz is used for a  $C/N_0$  of 45 and 30 dB-Hz respectively. Such bandwidths would not be attainable without aiding since the PLL lock threshold is reached for mere 8Hz, against 1Hz if aiding is used.

The influence of the TCXO oscillator error in the PLL causes an increase of the observable noise. For a PLL equivalent bandwidth of 40 Hz and without aiding, the carrier phase error reaches 3 mm and 7.5 mm for a  $C/N_0$  of 45 and 30 dB-Hz respectively, while if aiding is used the errors reach 2.5 mm and 6.5 mm respectively for that same filter bandwidth. It also causes the lock threshold to be reached for higher bandwidths than in the case when no oscillator error is present: the lock threshold is reached at 11 Hz in the case of unaided, against 4Hz in the case of aiding for a  $C/N_0$  of 45 dB-Hz. The PLL bandwidth related to the minimum error should be close to 18Hz in the case of aiding and 30Hz for the case of the unaided, corresponding to observation errors of approximately 5.5 mm and 7.5 mm respectively and for a  $C/N_0$  of 30 dB-Hz. Thus it can be seen that the TCXO forces an increase of PLL bandwidth from 8Hz to 18Hz when compared to the scenario where no oscillator error is present.

Therefore, for Level 4 integration the TCXO oscillator is a limiting factor for achieving better performances. To assess Level 5 integration, simulations were carried out for  $C/N_0$  of 45 dB-Hz and TCXO oscillator with 7.3 mm 1-sigma error. Results are shown in Table 3, where a reduction of 3 mm in the carrier phase error can be achieved using Level 5, an improvement towards the ideal case where no oscillator error would be present, for which the expected error would be 1mm.

Level 4 already tested with real live data in the IADIRA project [6], hence constitutes a more mature and better starting point for future research. Furthermore, the use of AltBOC already delivers quite high quality code observations when compared to GPS, and can still be improved using level 4 and level 5, which by itself is expected to contribute for better performances in urban mapping. Level 4 integration is selected for implementation in the ATENEA platform.

Figure 8 presents the baseline receiver code based positioning performances, considering an average scenario between 30 and 45 dB-Hz and that all remaining observable errors (tropospheric, relativistic, ionospheric, satellite clock and orbits) are cancelled using conventional techniques and also neglecting multipath effects. Note that the values presented do not reflect satellite outages. It is expected that the aiding will bring additional benefits in such cases, since the navigation filter shall be able to coast to the inertial sensor measurements during outages and the receiver would be able to quickly relock in case satellites are momentarily lost

	BW=40Hz, no aiding	BW=40Hz, aiding	BW=8Hz, aiding	BW=40Hz, no aiding	BW=40Hz, aiding	BW=18Hz, aiding
	w/o oscillator error			TCXO		
PLL error @ 45 dB-Hz	2mm	1mm	1mm	3mm	2.5mm	3 mm
PLL error @ 30 dB-Hz	7mm	6mm	3mm	7.5mm	6.5mm	5.5mm

**Table 3: Expected aided receiver performances based on code observables**

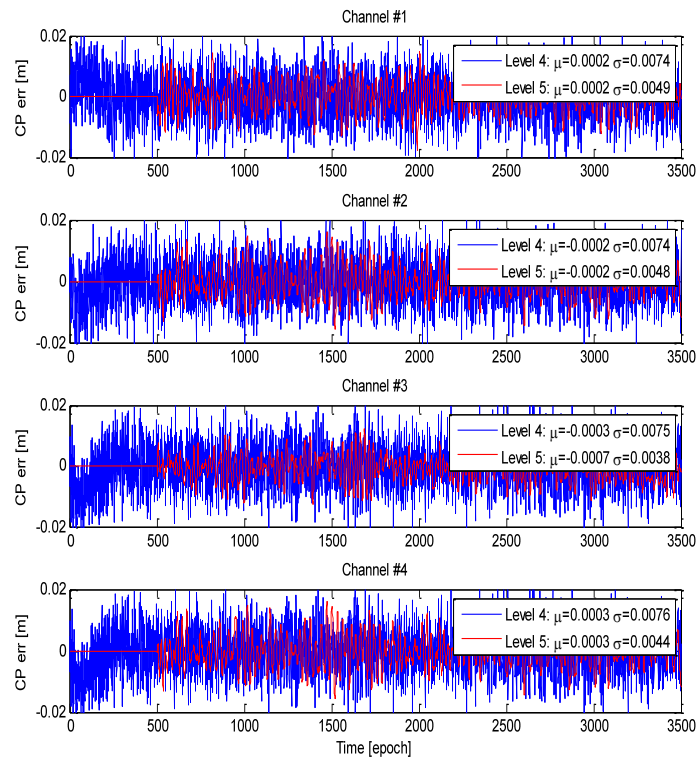


**Figure 8: Level 5 - Ultra-Tightly coupled hybrid GNSS-INS performances**

Signal	Code Error	Vertical Error VDOP=2.5	Vertical Error VDOP=4	Horizontal Error HDOP=2	Horizontal Error HDOP=3
Galileo E1 BOC(1,1)	0.5 m	1.25 m	2 m	1 m	1.5 m
Galileo E5 AltBOC(15,10)	0.1 m	0.25 m	0.4 m	0.2 m	0.3 m

**Table 4: Expected aided receiver performances based on code observables**



### 2.2.5. ATENEA Platform

Figure 9 shows the high-level overview of the ATENEA platform concept, specially designed to allow the development of an Integrated GNSS/INS/LiDAR navigation filter. The following elements are identified:

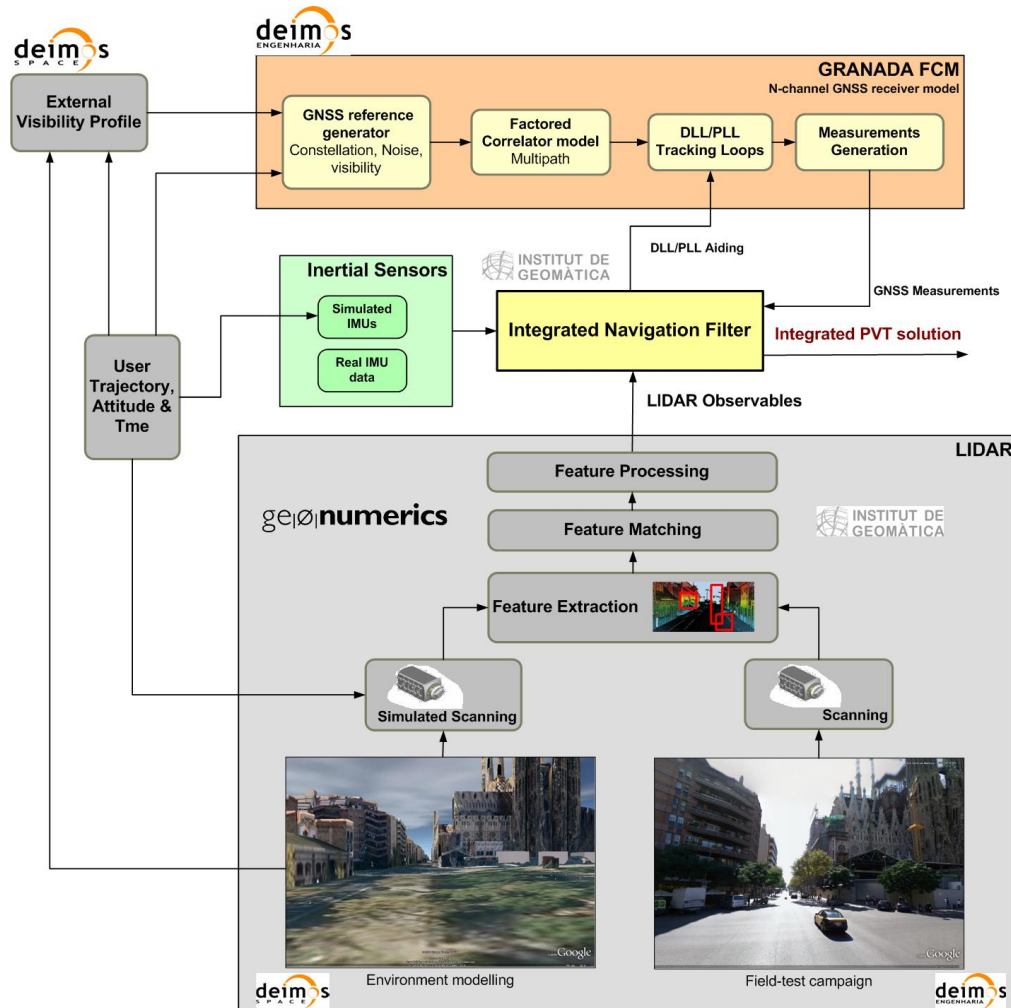


**Figure 9: ATENEA Platform concept**

#### ■ GNSS Receiver based on GRANADA FCM [10].

This module generates GNSS measurements according to the user trajectory, attitude, and time. It includes a GNSS constellation simulator, noise and multipath models, sampled-based tracking loops, and measurements generation. It provides GNSS observables to the integrated navigation filter and allows external tracking loops aiding. A visibility profile considering the defined environment is also fed to the GNSS model.

- *Inertial Sensors*: the navigation filter accepts both simulated and real collected IMUs data, in order to allow deep integration with the GNSS receiver.
- *LIDAR*: to provide LIDAR observables to the navigation filter, two options are envisaged: environment modeling, using available 3D models of streets to simulate LIDAR scanning in order to feed the feature extraction, matching and processing modules; and field-test collected data, in which real LIDAR measurements are obtained, providing cloud of points to the feature extraction, matching and processing modules.





- *Integrated Navigation Filter:* the key element of the ATENEA project is the development of an integrated GNSS/INS/LIDAR navigation filter capable of using the different input observables in the best possible way. The filter uses a deep integration approach (level 4) incorporating GNSS, INS and LiDAR measurements

The SW platform is based on the GRANADA FCM, which is a Simulink toolbox. Routines and functions in other programming languages can be integrated in the platform. Simulated data of real streets are obtained from Google Earth available models, allowing a fast preliminary development of the ATENEA software. A specific format is used to generate simulated scanned inputs to LIDAR processing functions. A common user trajectory and time is configured to feed and synchronise the GNSS platform, the inertial sensors and the LIDAR inputs.

The main objective of this platform is to assess the performance of the integrated Navigation filter in different scenarios, using both real and synthetic data of the different involved sensors.

Several adaptations have been performed in the FCM for the ATENEA platform:

- New block for AltBOC modulation
- Reference generation. A standardized user trajectory can be input to the model (standard XML trajectory files or GPX file)
- Upgrade for multiconsellation support
- External visibility profile, allowing to define a visibility matrix for each S/C vs time.
- Upgrade multipath models. Currently, the FCM implements a fixed statistical approach for urban users, in which the model parameters are fixed for all satellites. The model is updated in ATENEA for allowing time-variant satellite dependant multipath parameters, changing with time and position according to the user geometry. The direct path power is cancelled during the shadowing of a satellite by a building or other obstacle.

#### ▪ **Environment modelling and field-test data Collection**

The main task of the Environment Simulator is to gather the characteristics of the building environment to compute the satellite visibility, deciding the presence of a Line Of Sight (LOS) ray, and measuring the distance to the walls, needed to the LiDAR subsystem.

The building model should be as accurate as possible to represent with a high degree of fidelity the real environment that could be found when carrying out field measurements. A complete high-resolution measurement campaign would be very complex and costly, so the approach followed is to leverage the models that are available in the Google Maps™ and Google Earth applications.

Once the building model is obtained, the trajectory of the receiver is translated to the new reference frame and the vectors that define the rays from the receiver to the satellites are computed, as well as the satellites visibility. The scanning vectors for simulated LiDAR are also computed.

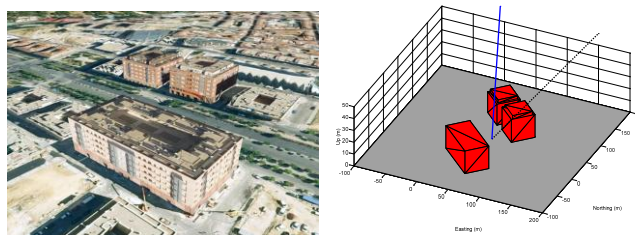


**Figure 10: Imported building environment (right) from Google Earth models (left)**



### ▪ **LIDAR modelling: feature extraction, matching, and processing**

LIDAR can be used to detect obstacles and measure the distances to surrounding objects. By using LIDAR, the same obstacles that obstruct GNSS signals can be used to estimate changes in the receiver position. This was the concept explored in [11], where an integration filter was used to merge inertial data with GPS and laser scanner measurements in order to determine the receiver's delta position. This approach provides enough measurements which could be used for continuous navigation in urban environment.

Different stages are necessary to process LiDAR information, which is composed of time tag, raw data, laser point coordinates and feature ID: preprocessing, feature extraction, feature matching, and observables generation.

The most common 3 D feature in LiDAR is the planar surface, which is shaped by a cloud of points. A plane is characterized by a vector normal to plane surface and the distance of plane. The steps in the plane extraction start with the registration of 3D points in a 3D. Then the accumulation of points is analysed, and if the criteria conditions are met, the feature is declared as a plane. This can be done through a Hough transform analysis. Then a morphological analysis is needed for points filtering. Finally, a least square adjustment with a plane model is performed for the extraction of plane parameters.

For plane matching, information coming from the different sensors is used. Plane matching involves an accurate estimation of plane parameters, all the points concurrent to a plane are needed, and adjusted with a least-square method. The correcting angles are computed with coplanar cloud points through least-squares adjustment. The system solution gives the correcting pair angles. The observations are then computed based on the direct and inverted LiDAR geometry equation:

The selected LiDAR instrument output data are in local reference frame (UTM). They must be transformed into WGS84 and range-angle pair for their integration in the navigation filter. The set of LiDAR points classified into planes they belong; this classification is performed for only the first time points were acquired by each sensor. They are matched with the INS/GNSS orientation instrument postprocessed tPVA trajectory.

### ▪ **Integrated navigation filter**

The NAVEGA navigation filter integrating GNSS, INS and LiDAR is being developed by the Institute of Geomatics. The NAVEGA will overcome some limitations of the traditional Kalman filter EKF and Extend Kalman Filter EKF approaches, such as the well known numerical stability issues (which are not so critical), the non-support for more than one dynamic model or the stochastic-functional link to “dynamical” observations through  $C_{x-x}$ . In addition, the Kalman-based filters are designed for a Gauss-Markov explicit Least Square formalism  $l+v = h(x)$ , with no support for the more general Gauss-Helmert  $g(l+v, x) = 0$ .

Therefore, with NAVEGA the key aspects tackled are:

- separate estimation from modeling
- group models in loadable “modelboxes” or “toolboxes”
- allow for redundancy both for dynamic and static models
- use of numerically stable linear solvers
- both in the dynamic and static observation equations, access observations and states/parameters by reference
- use of differential nav & pos models does not necessarily lead to “single” or “double differenced” measures
- being conservative on the assumptions and being generic

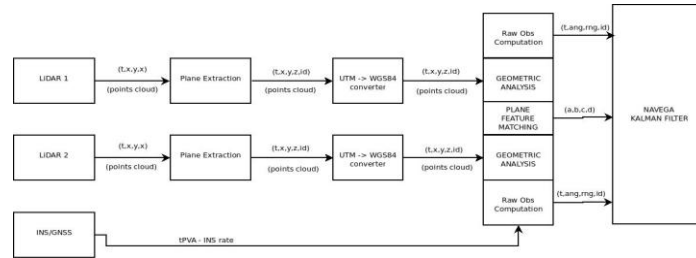


**Figure 11: LiDAR processing for integration in the navigation filter**

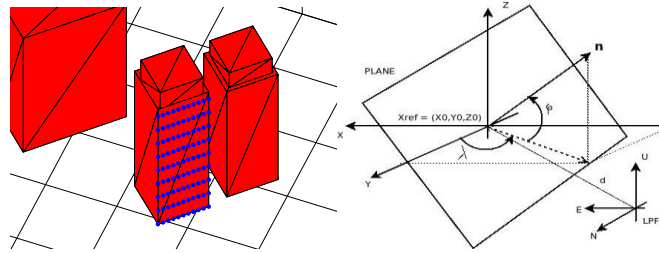


**Figure 12: Point cloud resulting of the LiDAR scanning and plane location**

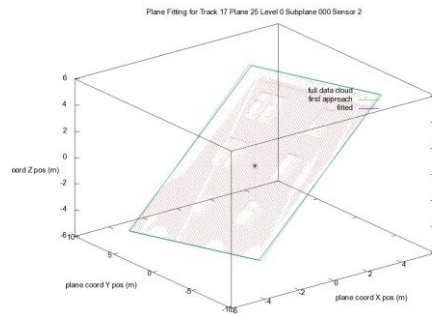


**Figure 13: Plane matching**

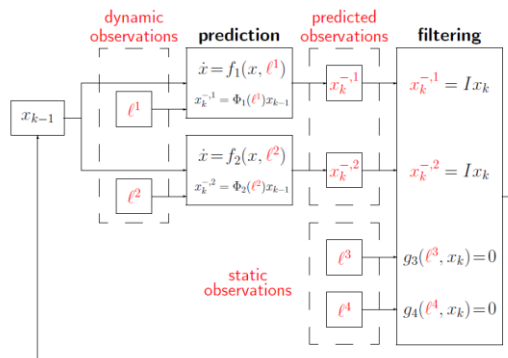


**Figure 14: NAVEGA filter architecture**

The NAVEGA SW platform is able to incorporate additional modelboxes or toolboxes as DLL, and different navigation strategies.

Concerning the estimation filter, two numerical LS implementations are considered, based on SRIF or QR.





### 2.2.6. VALIDATION

The GNSS receiver model used in the ATENEA platform has been validated comparing its results with experimental data obtained using an FPGA-based hardware receiver (Figure 15). The validation tests, performed in open loop, focused on the effects of Carrier-to-Noise Density Ratio; Output Noise Cross-Correlation; Influence of Code Delay Error in the Outputs; Influence of Doppler Error in the Outputs.

The tests proved that the GRANADA FCM can be used to accurately simulate a HW receiver.

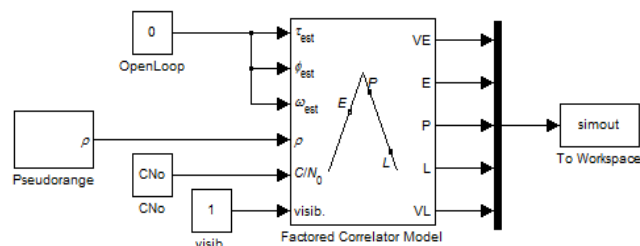


Figure 15: Experimental receiver (top) and receiver model (bottom)

#### Validation with synthetic data

An extensive simulation campaign has been performed using ATENEA platform, to validate the results in different scenarios. Table 5 provides a summary of the considered scenarios. For each case, results from different integration levels are obtained to verify that the additional of additional sensors improves the navigation solution, which is the main outcome of these test campaign:

- PVT solution using GNSS observables
- PVT solution using GNSS+INS observables
- PVT solution using GNSS+INS+LIDAR observables



ID	Scenario	User	Location	Description
S1	Urban Canyon	Vehicle (50 KM/h)	Broad Street, lower Manhattan, NYC	Very limited satellites LoS. Extreme multipath.
S2	Urban	Vehicle (50 KM/h)	Santa Engracia, Madrid centre	Limited satellites LoS High Multipath
S3	Suburban	Vehicle (50 KM/h)	Avd. Asturias, Madrid	Quite open sky, small trees. Moderate Multipath
S4	Tree-shadowed	Vehicle (50 KM/h)	Avd. Asturias, Madrid with added trees	Trees along road sides LoS and Multipath affected by trees

**Table 5: Validation Scenarios (synthetic data)**



**Figure 16: Urban Canyon Scenario (S2 in Table 5)**

▪ **Field test data collection campaign.**

On 6-7<sup>th</sup> September 2011, a field data collection campaign was carried out at Dormund (Germany). The objective was to assess the ATENEA concept in real environments using real GPS, LIDAR and IMU observables. The test scenario was selected so that the test vehicle followed a pre-defined trajectory along a 1.7 Km long closed path. The path, shown in Figure 17, covers an urban environment, with two lane streets and 4-storey buildings. Buildings' fronts are mainly planes parallel with respect to the axis of the streets. Some lampposts and trees are present as features of the streets. There are areas of narrow streets ("urban canyon"), as highlighted in the figure. The figure shows the reconstructed trajectory. Green dots indicate good GPS visibility and measurements accuracy, while red dots corresponds to areas in which GPS quality is degraded due to poor visibility and multipath.

The test was carried out using TopScan equipment for Mobile Mapping, which is shown in Figure 18. The TopScan Multivan is equipped with two Lynx LiDAR sensors, a Litton LN-200 IMU, and a Trimble Zephyr GPS antenna. For the tests, an active splitter was added to allow the use of a GPS L1 Intermediate Frequency (IF) data recorder.

The following measurements were recorded: LiDAR measurements, IMU raw data, odometer raw data, postprocessed tPVA (time-position-velocity and attitude), GPS raw data and GPS IF data.

For the reference trajectory computation, 3-cm accuracy is required for plain and height coordinates. This is achieved by an indirect method based on known control points in the LiDAR point cloud, which is fitted to these geo-referenced points. A survey office has been subcontracted for geo-referencing the control points, which are high contrast points in a save place beside the traffic.



Measurements recorded in the data collection campaign have been post-processed for synchronisation of all collected data. The GPS IF samples are processed to derive the Auto Correlation Function (ACF) using a specifically developed SW tool. The GRANADA FCM models the ACF characterised using recorded GPS IF samples, generating proper GNSS observables. The GNSS receiver model is tuned according the user trajectory, satellites constellation, visibility profile, estimated multipath model, and ACF shape (obtained from post-processing on recorded IF data).

The LiDAR measurements have been also used for multipath characterization in urban environment, using information on the 3-D environment determined by the LiDAR measurements. Measurements likely to be affected by multipath will be excluded from the navigation filter.

Mixing real recorded data and simulated GNSS receiver observables, the integrated navigation algorithm provides the PVT solution. The results compared with both simulated data, the PVT solution in the stand-alone GPS receiver available in the test vehicle, and the reconstructed trajectory provided by the TopScan system show the improvement in the solution offered by the ATENEA integrated filter.



**Figure 17: Imported Field test data collection campaign path**



**Figure 18: TopScan experimental setup**



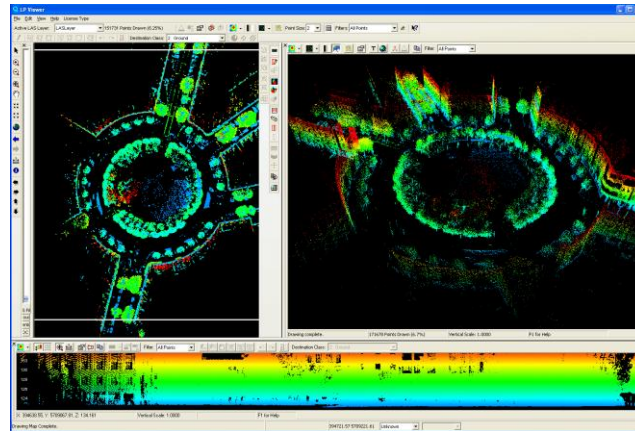


Figure 19: Collected LiDAR data

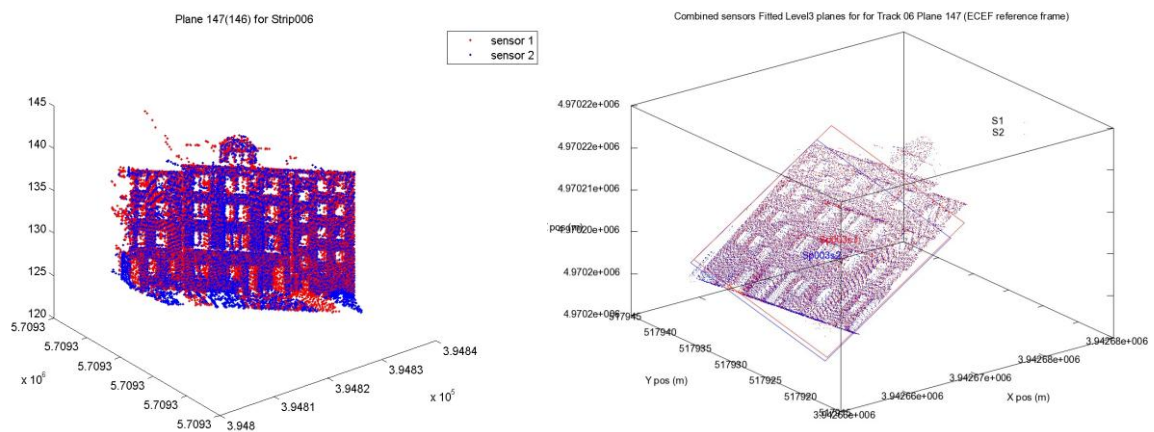


Figure 20: Example of LiDAR pre-processed data from Dortmund campaign after the primary plane extraction (left) and extracted geometrical planes (right)

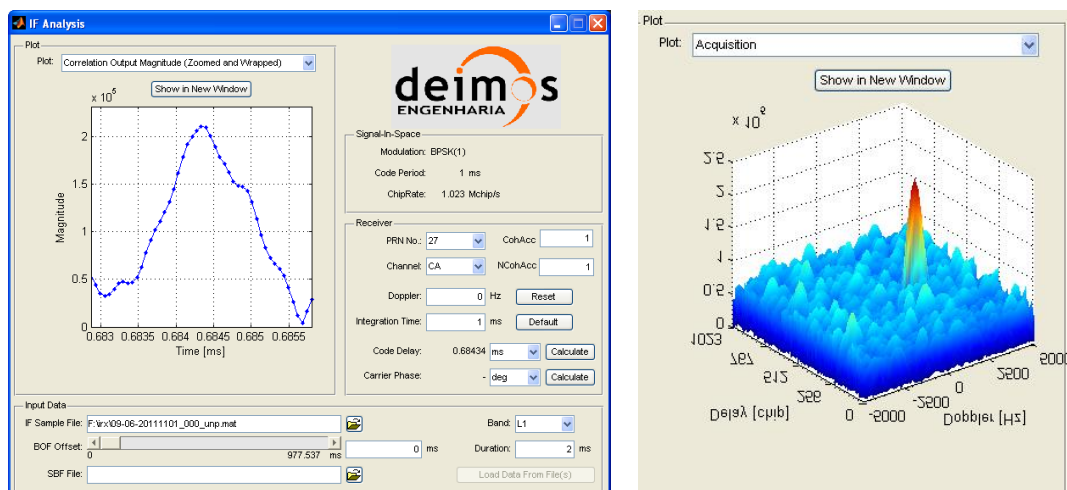
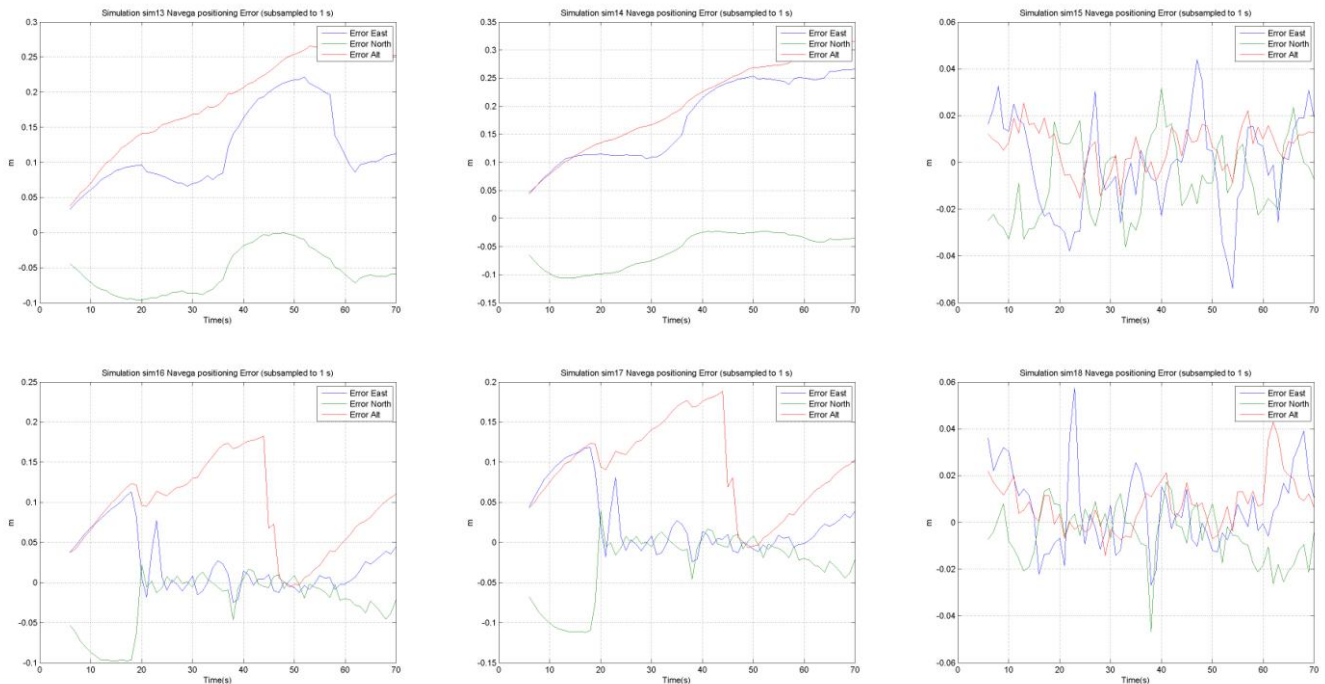


Figure 21: ACF derivation from IF data



### 2.2.6.1. Simulation results in suburban environment

Results of simulation in urban environment can be observed in Figure 22. In this composition, from left to right, the E1Cboc, the L1TmBoc and the E5AltBoc modulations are shown in each column. On the same composition, from top to down, the upper row represents the results with inertial aiding and Doppler feedback (without LiDAR) and the lower row shows the results with inertial aiding, including Doppler feedback, and LiDAR.



**Figure 22: simulations results in sub-urban environment**

It can be observed the effect of satellite occultation caused by the surrounding buildings and the modelled multipath for modulations E1Cboc and L1TmBoc. There is a noticeable increment in the **error** of the navigation solution that it is **completely mitigated in the horizontal component with the utilization of the LiDAR observations**.

It is observed that **multipath and satellite occultation has no apparent effect on E5AltBoc modulation, which offers excellent performances**, as expected. Therefore, in this case there is no observable improvement of the navigation solution when the LiDAR is applied.



### 2.2.6.2. Simulation results in urban environment

This group simulates the urban and suburban scenarios. The results of these simulations are shown in Figure 23 where the plots on the top row are the results without LiDAR, the middle row represent the results with LiDAR and the bottom row is the East-North profile of each of the scenarios. From left to right the scenarios are the S4 Tree Covered, the S2 Urban, and the S1 Urban canyon ones.

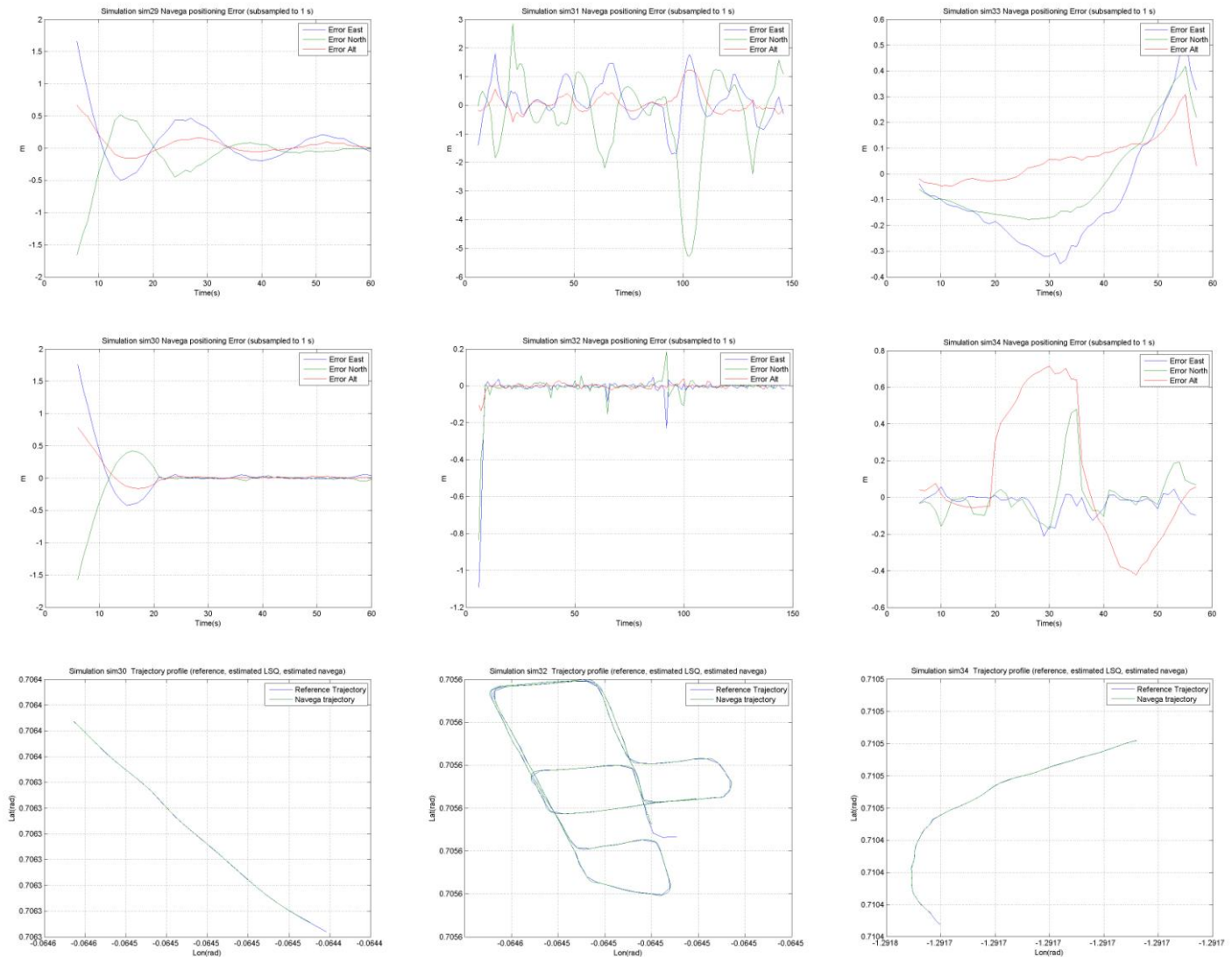


Figure 23: simulations results in urban environment.

For the S4 **tree covered scenario**, it can be observed the effect of trees on the navigation solution as changes in the accuracy with time. **When the LiDAR is used**, these changes are reduced and the **accuracy is then improved** as expected.

In the S2 **Urban scenario**, it was simulated the run of a vehicle along different streets that run North-South and East-West. When no LiDAR is used, changes of position accuracy are clearly observed caused by **changes of the visible satellite configurations because of the different travel directions**. **When the LiDAR is used, the effects of the changes are clearly removed from the navigation solution and the accuracy is clearly improved**.

For the S1 **Urban canyon scenario**, the scenario simulated a van running along an avenue surrounded by tall buildings. The change in direction of this avenue was very smooth; therefore it is not observed a change direction effect like in the case of the S2 Urban scenario because the satellite configuration was very stable. **When the LiDAR was used in the scenario, it is clearly observed how the accuracy was improved for the horizontal position**. The effects on vertical accuracy are expected because of the reasons given before.

In order to not increase too much the number of simulations, only simulations with E5AltBoc modulation were performed.

### 2.2.6.3. Simulation results with low-cost hardware

With this case, hypothetical performance of a system based on a more economic hardware (2000 € for a MEMS IMU and 30000 € for a low-end LiDAR system, TCXO clock), in strong multipath conditions and with signal shadowing, has been checked. The results of such system can be observed in Figure 24. The obtained accuracy is quite acceptable (overall when the SV is aiding the GNSS), reaching an RMS error of less than 30 cm. IMU calibration achieved and kept despite of the satellite shadowing. These results show the possibilities of using low cost aiding sensors with Galileo E5AltBoc modulations.

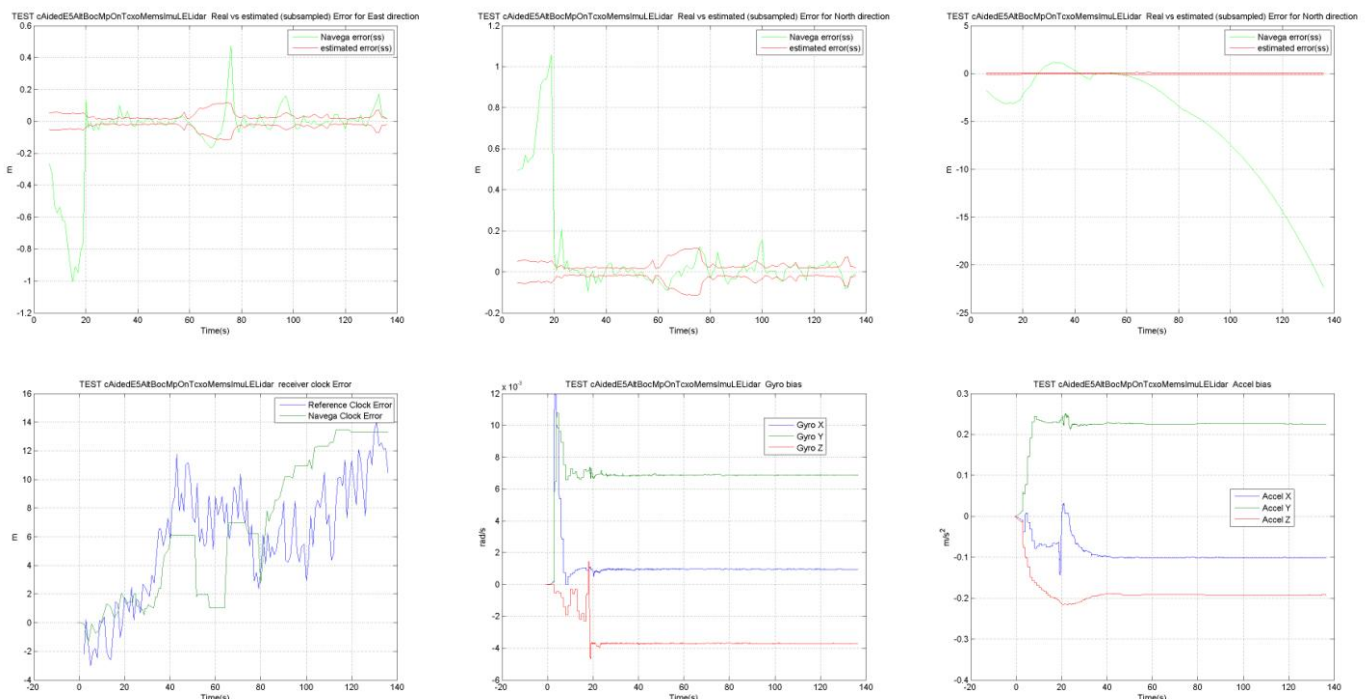


**Figure 24: low cost sensors simulations**





#### 2.2.6.4. Results from real dataset

In this case, the results have been obtained not with simulated but with **real datasets** from the LiDAR and the IMU instruments. The results of this group can be observed in Figure 25. Left column corresponds to E5AltBOC modulation while right column corresponds to GPS L1 BPSK. Upper row does not include LiDAR in the navigation filter; its effect is shown in the lower row. It has to be mentioned that a strong multipath component has been included in the tests, following the IF analysis; probably multipath has been overestimated. By that reason the error of the L1BPSK with no LiDAR is so high.

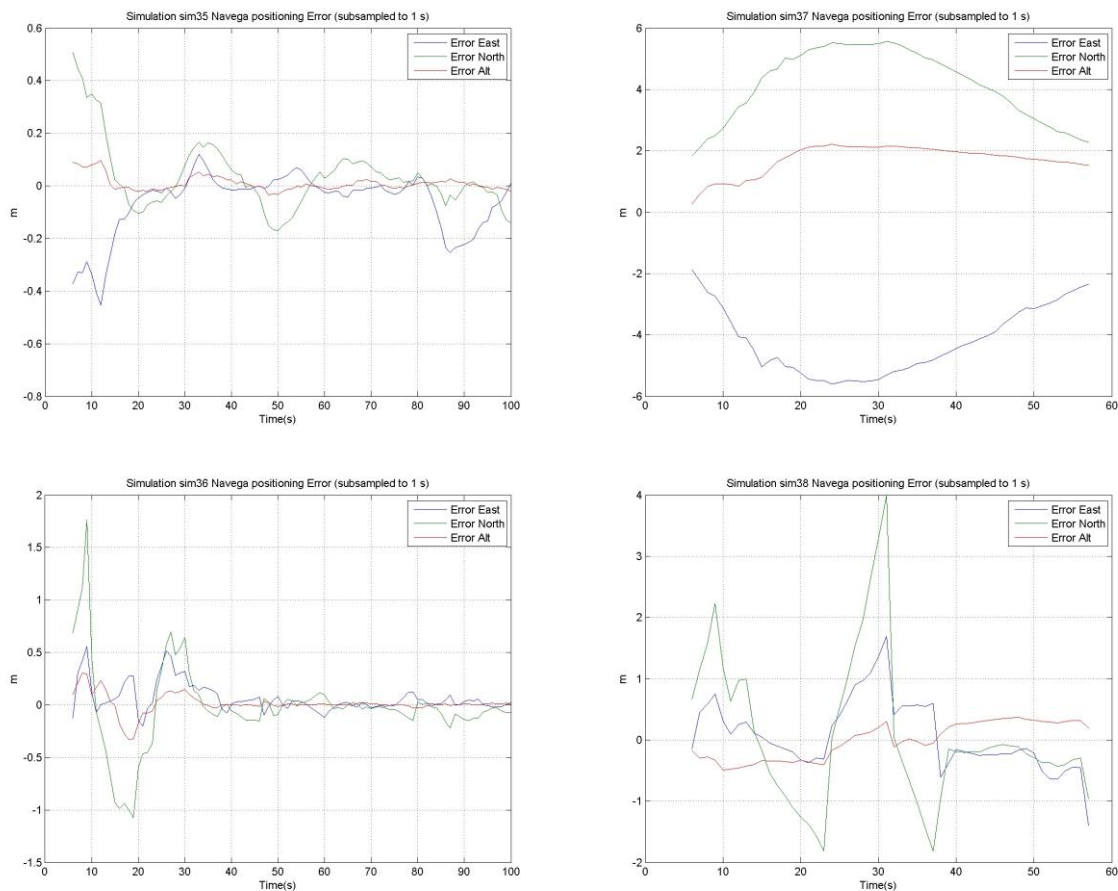


**Figure 25: results from real datasets**

It is also observed that the **performance of the E5AltBoc modulation with real IMU and LiDAR datasets are quite good**. It is also observed the effect of the LiDAR on the results; but apparently it seems it does not improve too much. Some of the causes it is believed this happens is because of the **reference trajectory** used. This trajectory **was obtained with an INS/GPS subsystem** and despite of the quality of the system, **some residual effects still may be present**. In addition to this, it must be taken into account that **the LiDAR sensor must be calibrated**. Despite special care has been intended in the calibration of the LiDAR, the internal optical model is a black box, and the **misalignment adjustments** may be not totally accurate. However the **results obtained are acceptable** and may be included within the second grade of precision (intermediate accuracy applications).





#### **2.2.6.5. Multipath characterisation using LiDAR**

The data collected in the field test campaign have been used to characterise multipath error in urban environments with the help of LiDAR. GPS IF raw measurements have been processed with coupled amplitude delay lock loop (CADLL), which is a multipath estimating architecture. The LIDAR is able to provide the information about the structure of surrounding objects e.g. buildings, trees, poles etc. and their distance from the receiver, so this information helps in predicting the possible multipath if the receiver is in the "vicinity" of the objects.

The multipath found is of low power and remains for short intervals. The portion of test environment where multipath was found is marked with red points in Figure 26. The yellow points mark the path followed during the test. This leads to the conclusion that for this particular data collection, the environment has produced scattered multipath. There are intervals on the other side with important signal attenuation or signal blockage, which should be considered for multipath analysis scenario as a remark for the future work; a reflective and specular multipath is more desirable from the analysis point of view. Also, it is important to consider that LIDAR provides information about coordinates of planes but it does not provide details about the type of the surface. So, it is not trivial to estimate just from LIDAR information if the multipath ray is a strong reflection or just a scattering. Finally, the front-end used is of low bandwidth (IF frequency was 4.12 MHz; sampling frequency was 16.3676 M Hz. The data was recorded at the rate of 2 bits per sample with 2 quantization bits); higher bandwidth front end would have improved the analytical capacity.

As recommendation for the future, further data collection campaigns are required, with higher end equipments (in particular Fron-End), and in well characterised environment (eg free of trees so shadowing effects do not mask multipath).



**Figure 26: Part of the track in which multipath was found (red points)**



## 2.3. Conclusions

The ATENEA project has developed an advanced concept for seamless navigation at the cm-level regardless of the environment based on the following technologies:

- **Deeply coupled GNSS/INS receiver design.** There is a clear improvement in the navigation solution for tightly coupled approaches. **The more coupled are the INS with the GNSS, the better is the accuracy.** Thanks to the Doppler feedback it is possible to keep and recover the tracking of the satellites in shadowing conditions
- **Galileo signal capabilities.** The **Galileo E5AltBOC signal offers excellent performances in all conditions.** This modulation opens a field for professional GNSS applications with unprecedented accuracy.
- **Integrated GNSS/INS/LIDAR navigation filter.** An innovative unique integrated navigation solution for the integration of observables from GNSS, IMU, and laser sensors is proposed, allowing to reduce the costs of the currently expensive equipment in these applications. The use of LiDAR measurements in the navigation filter results in a huge increase of performance in urban environment, especially in the horizontal component.

The proposed algorithms have been tested in the ATENEA platform SW environment, developed upon the GRANADA simulator. A field campaign with real data has been carried out. The ATENEA technologies have been thus investigated down to a pre-industrialized solution ready to be integrated in professional applications.

Almost ATENEA objectives have been met. However, the initial objectives of the field test campaign have not been fully achieved. In the project plan, it was foreseen to use Galileo early signals (IOV satellites) in the field test campaign, but unfortunately it was not possible due to the delay in the Galileo programme, and only GPS L1 C/A data was used.

Concerning multipath, the goal of using LiDAR as a multipath rejection device has not been fulfilled. While characterising multipath in urban environment using LiDAR data remains an important research topic, the effort and budget allocated in ATENEA for this task was clearly not sufficient.

## 2.4. Public website address and relevant contact details

<http://atenea.deimos-space.com>

Antonio Fernández

[antonio.fernandez@deimos-space.com](mailto:antonio.fernandez@deimos-space.com)

+34 91 806 34 54

DEIMOS Space SLU

Ronda de Poniente, 19;

28760 Tres Cantos (MADRID) – SPAIN



*End of document*